Journal of Molluscan Studies
February 2019, Volume 85, Issue 1, Pages 154-165
https://doi.org/10.1093/mollus/eyy061
https://archimer.ifremer.fr/doc/00479/59048/

Revisiting the *Lepetodrilus elevatus* species complex (Vetigastropoda: Lepetodrilidae), using samples from the Galápagos and Guaymas hydrothermal vent systems

Matabos Marjolaine [1, *], Jollivet Didier [2]

[1] IFREMER, Centre de Bretagne, REM/EEP, Laboratoire Environnement Profond, Plouzané, France
[2] Sorbonne Université, UPMC Univ. Paris 06, CNRS UMR 7144, Adaptation et Diversité en Milieu Marin, Equipe ABICE, Station Biologique de Roscoff, Roscoff, France

* Corresponding author : Marjolaine Matabos, email address : marjolaine.matabos@ifremer.fr

Abstract :

The current distribution ranges of vent species result from the complex tectonic history of oceanic ridges. A growing number of DNA barcode studies report the presence of cryptic species across geological discontinuities that offset ridge systems and have gradually helped to draw a more precise picture of the historical migration pathways of vent fauna. We reexamined the phylogeny of species within the *Lepetodrilus elevatus* complex along the East Pacific Rise (EPR) ridge system in the light of new samples from the Galápagos Rift and the Guaymas Basin. Our analyses of mitochondrial cytochrome c oxidase subunit I gene sequences, coupled with morphological data, highlight the occurrence of a distinct lineage along the Galápagos Rift and offer new insight into the current distribution range of this species complex. Due to the absence of clear morphological diagnostic criteria and the potential overlap of these lineages at key locations, we recommend reassigning the taxon *L. galriftensis* to the subspecies level and maintaining the name *L. elevatus* for all clades along the EPR/Galápagos Rift system.

INTRODUCTION

Biodiversity conservation represents the most challenging issue for scientists and policy makers today, therefore determining current species' ranges is of utmost importance (Hendry *et al.*, 2010). Understanding hydrothermal vent biogeography is, however, often hindered by the lack of samples at key areas along ridge systems. The growing literature on vent phylogeography reveals a complex history of lineages at hydrothermal vents, where the constant reorganization of ridges and geodynamics affect gene flow over time (Vrijenhoek, 1997; Jollivet, Chevaldonné & Planque, 1999). Continuous changes in ocean floor geomorphology, such as ridge reorganization/fossilization (Mammerickx & Klitgord, 1982), or their subduction under volcanic arcs or continental plates (Tunnicliffe & Fowler, 1996), make identifying biogeographical patterns difficult, simply because species' ranges evolve with the creation and subsequent removal of physical barriers to gene flow (Plouviez *et al.*, 2013). The present distribution of vent fauna is a result of these historical events, modulated by the life-history traits of each species, which determine the potential for colonization of more or less distant territories through larval dispersal (Marsh *et al.*, 2001; Mullineaux *et al.*, 2002, 2010; McGillicuddy *et al.*, 2010). In addition, geographical distances between neighboring vents and habitat density mainly depend on the ridge spreading rate (Hannington *et al.*, 1995) and the convection of heat, according to the oscillations of the magmatic chamber beneath the ridge (Watremez & Kervevan, 1990). Hydrothermal fluid circulation, directly determined by magmatic and tectonic activity, controls the rate of appearance and disappearance of vent sites (Vrijenhoek, 1997; Jollivet *et al.*, 1999). These local dynamics influence the temporal dynamics in communities through ecological succession patterns (Shank *et al.*, 1998; Marcus, Tunnicliffe & Butterfield, 2009). In highly unstable portions of ridges (i.e. segments with the highest accretionary

rates), vent communities rarely reach the climax state. Thus, position in the ecological succession order (i.e. early, mid and late successional colonizers) strongly influences species' distributions. It also influences the number and size of populations, and therefore the effective population size (number of reproductive adults) of species and the number of offspring able to colonize new sites (Vrijenhoek, 2010).

There is a need for knowledge on biodiversity and distribution of vent species, in order to describe and understand biogeographical patterns and the history of vent colonization. Over the last decade, a growing number of DNA-barcoding studies have reported the presence of well-separated cryptic species across physical geological discontinuities that offset ridge systems, particularly along the well-studied East Pacific Rise (EPR) (Johnson *et al.*, 2008; Plouviez *et al.*, 2009; Matabos *et al.*, 2011) or in the northeastern Pacific Ocean on both sides of the Blanco Transform Fault Zone (Johnson *et al.*, 2006). The occurrence of cryptic species able to migrate over great distances and hybridize at some locations, impedes our ability to define clear-cut biogeographical provinces along the EPR (Matabos *et al.*, 2011). Species' distributions along the EPR are thus far from being understood and clarifying them may change our perception of East Pacific biogeography.

Based on biogeographical studies using species presence/absence, the EPR was originally considered as a single biogeographical province (Tunnicliffe, 1988; Tunnicliffe & Fowler, 1996; Bachraty, Legendre & Desbruyères, 2009). However, Matabos *et al.* (2011) recently demonstrated that the southern EPR represents a transition zone between the northern EPR and the Pacific-Antarctic Ridge, where several physical barriers prevent larval dispersal and promote species partitioning. In this specific context, tectonic events, creating physical barriers such as transform faults

or the Easter/Bauer microplates, may have played a crucial role in the allopatric isolation of species. A large number of taxa, including gastropods, polychaetes and bivalves, indeed display population divergence on either side of the Equator and/or the Easter microplate, generating cryptic species complexes along the 5000 km of the EPR (Won *et al.*, 2003; Hurtado, Lutz & Vrijenhoek, 2004; Matabos *et al.*, 2008; Plouviez *et al.*, 2009). Several geological events related to the major reorganization and re-orientation of the EPR over the last 20 Myr likely coincided with the timing of the estimated genetic divergences. Population divergences in the majority of taxa likely occurred during two distinct events about 11 and 1.3 Ma, respectively (Plouviez *et al.*, 2009), corresponding to the rotation of the Bauer microplate, the reorganization of the Mathematician Ridge (for the older date) and the setting up of the most pronounced transform faults that offset the ridge between 9°50'N and 7°25'S (for the more recent date). Estimations of divergence dates (0.7 to 3.5 Ma) from a multilocus approach also indicate that part of the observed genetic divergences between the southern and northern populations of the vent mussel *Bathymodiolus thermophilus* at the Equator may derive from the formation of the Easter microplate, about 3 to 5 Ma, via allele introgression through this older, but semipermeable barrier (Plouviez *et al.*, 2013).

Among taxa exhibiting cryptic species, the *Lepetodrilus elevatus* species complex is one of the most genetically diversified, with at least three distinct genetic units emerging from the ridge-system reorganization. Species in this complex, similar to all species of *Lepetodrilus*, possess planktonic, presumably lecithotrophic, larvae (Berg, 1985; Tyler *et al.*, 2008). As originally described, *Lepetodrilus elevatus* contained two morphologically distinct subspecies: *L. e. elevatus* from the EPR and *L. e. galriftensis* from the Galapagos Rift (McLean, 1988). These limpets are very abundant on the tubes of the tubeworm *Riftia pachyptila* and on mussel shells, along the EPR and the

Galápagos Rift. On the EPR, the species is composed of at least two cryptic lineages between 21°N and 21°S, which co-occur at 9°50'N where they are likely to hybridize (Matabos *et al.*, 2008). This population split has been hypothesized to have been driven by the transient formation of the Bauer microplate located between 10° and 15°S over the last 15 Myr (Matabos *et al.*, 2008) and/or with the reorganization of the Mathematician Ridge about 11 Ma (Plouviez *et al.*, 2009). The emergence of a secondary contact zone prevents the exact positioning of the geographical barrier. Based on shell morphology, Craddock, Lutz & Vrijenhoek (1997) and Johnson *et al.* (2008) proposed that these lineages represented true distinct species, and therefore elevated *L. e. galriftensis* to the species level (Craddock *et al.*, 1997) and attributed one of these cryptic lineages to *L. galriftensis* (referred to as *L.* aff. *galriftensis*; Johnson *et al.* 2008), but the absence of specimens of the Galápagos Rift morphotypes did not allow the authors to confirm this hypothesis. This species assignment was then challenged by Matabos *et al.* (2008), who showed that both EPR lineages have a distinct shell biometry when compared with the reference (formalin-preserved) specimens of *L. e. galriftensis* sampled at Rose Garden (Galapagos Rift) in the early 1980s (McLean, 1988).

Another closely related species, *L. guaymasensis*, discovered on sulphide rocks and vestimentiferan tubeworms in the Guaymas Basin in 1984 (McLean, 1988), differs from *L. elevatus* in its size, and in its recurved apex that it shares with *L. fucensis* from the Juan de Fuca Ridge. Though morphologically different, there are no molecular data that confirm the occurrence of distinct species between the Guaymas Basin and the EPR.

In this study, we revisit the phylogeny of the *L. elevatus* species complex

together with other *Lepetodrilus* limpet species, in the light of new DNA barcoding data gained from ethanol-preserved samples from the Galápagos Rift and the Guaymas Basin.

MATERIAL AND METHODS

Collection of samples

Specimens of *Lepetodrilus elevatus galriftensis, L. pustulosus* and *L. tevnianus* were collected from the Galápagos Rift (0°46'N, 85°54'W) using the ROV *Hercules* onboard the E/V *Nautilus* in July 2015 (Table 1; Fig. 1). Specimens of *L. guaymasensis* were collected from cold seeps at Sonora margin in the Guaymas Basin (27°35'N, 111°28'W) using the HOV *Nautile* onboard the R/V *L'Atalante* during the BIG cruise in June 2010 (Fig. 1). After sampling, individuals were stored in ethanol until DNA extraction. All shells were kept for morphological analyses.

Molecular analyses

DNA was extracted from the whole body and purified using the 2% CTAB-1% PVP protocol adapted from Doyle & Doyle (1987) for alcohol-preserved specimens by Jolly *et al.* (2003). Partial sequences of the mitochondrial cytochrome *c* oxidase subunit I gene (mtCOI) were amplified with the universal primers LCO1490 and HCO2198 (Folmer *et al.*,1994) and/or nested specific primers obtained from a COI alignment of lepetodrilid sequences (COI-R: 5'-TAACTTCAGGGTGACCAAAAAATCA-3'; COI-F: 5'-GTTCAAATCATAAAGATATTGG-3'; Matabos *et al.*, 2008). About 100 ng of template DNA was amplified in a 50-µl amplification mixture containing 1x PCR buffer, 2 mM $MgCl_2$, 0.3 µM of each primer, 25 µM of each dNTP, 1U UptiTherm^{TM} Taq DNA polymerase. Polymerase chain reactions (PCR) were performed as follows:

(1) a 3 min initial denaturation step at 95 °C, (2) 35 cycles of 1 min of denaturation at 95 °C, 45 s of annealing at 50 °C and 2 min of elongation at 72 °C and (3) a 10 min final elongation at 72 °C. The PCR products were purified and sequenced on an ABI 3100 using the BigDye terminator chemistry (Applied Biosystems) following the manufacturer's protocol. Sequences were proofread and aligned manually using BioEdit Sequence Alignment v. 7.0.1.

To reconstruct the phylogenetic relationships between the northeastern and East Pacific species of *Lepetodrilus*, we used unique haplotypes of individuals belonging to each of the clades within the *L. pustulosus*, *L. tevnianus* and *L. elevatus* species complexes (Johnson *et al.*, 2008; Matabos *et al.*, 2008; Matabos *et al.*, 2011). Unique haplotypes of additional individuals from the Guaymas Basin (Johnson *et al*., 2008; present data) and other species collected at the Galápagos Rift (i.e. *L. pustulosus, L. tevnianus*) were added to the analyses together with sequences from the EPR of closely related species within the same genus, including *L. cristatus, L. fucensis* and *L gordensis* (Table 2; Fig. 1). To root the tree, we used *Gorgoleptis spiralis*, a species within the same family, Lepetodrilidae, as the most appropriate outgroup (Matabos *et al.*, 2008). With the exception of the sequences of Galápagos and Guaymas specimens (GenBank acc. nos MH458083 to MH458170), all sequences were obtained from the GenBank sequence repository.

Tree reconstructions were performed using the Bayesian inference (BI) and maximum-likelihood (ML) methods, with a final alignment made of 72 unique haplotype sequences of a 521-bp fragment of mtCOI. First, the best-fit substitution model was selected, using the BI criterion implemented in Modeltest v. 3.07 (Posada & Crandall, 1998). Both reconstruction analyses were then run using the selected Hasegawa, Kishino & Yano (HKY) model with a fixed gamma distribution and a

proportion of invariable sites (HKY+I+G) following the BI criterion values. BI analyses were performed using MrBayes v. 3.2.6 (Ronquist & Huelsenbeck, 2003), which uses a Markov chain Monte Carlo (MCMC) method for exploring the parameter space in a stepwise fashion. The analysis, involving four chains, was run for 1,000,000 generations with a sampling frequency of 1,000 and a burn-in of 10,000 trees. The ML tree was constructed using PhyML via the phylogeny.fr platform (Dereeper *et al.*, 2008). The ML analysis was performed following a heuristic search using the bioNJ tree as the initial tree and a NNI branch swapping process. Bootstrap support values were calculated based on 500 resamplings of the dataset. The trees were visualized using FigTree v. 1.4.2 (http://tree.bio.ed.ac.uk/software/figtree/).

Pairwise K2P distances (Kimura, 1980) were calculated between clades identified using MEGA7 software (Tamura *et al.*, 2013) to estimate the time since divergence between the newly sampled geographical lineages of *L. elevatus* and *L. tevnianus* following calibration times previously used by Johnson *et al.* (2006). To calibrate time since divergence (and the associated confidence interval, CI), a tree was generated using the RelTime-ML function implemented in MEGA7 using some expected splitting dates. These major tectonic events were (1) the subduction of the Farallon Ridge under the North American Plate between 28 and 25 Ma when considering the separation of the closest relatives *L. gordensis* and *L. guaymasensis*; (2) the formation of the Blanco Transform Fault Zone separating the axes of the Gorda and Juan de Fuca ridges, initiated 5 to 7 Ma, to calibrate the time elapsed since divergence between *L. fucensis* and *L. gordensis*; (3) the separation of the Guaymas Basin system from the EPR between 12.5 and 11 Ma (Mammerickx & Klitgord, 1982) and (4) the formation of the Easter microplate between 5 and 2.5 Ma to calibrate time since

divergence between *L. pustulosus* and the southern clade *L.* aff. *pustulosus* (Naar & Hey, 1991; Johnson *et al*., 2008).

Morphometric analyses

Morphometric measurements of the shells of the 82 newly sampled individuals from the Galápagos Rift (*Nautilus* Expedition 2015) for which we obtained mitochondrial DNA sequences were compared with data already published by Matabos *et al.* (2008). These data included the two cryptic lineages identified along the EPR and 85 shells of formalin-preserved *L. e. galriftensis* paratypes from the Galápagos Rift (collection from Los Angeles County Museum of Natural History; LACM 2528) for which DNA sequences were not available. Only the cryptic lineages of *L. elevatus* and *L. e. galriftensis* were included, because all other species can easily be identified based on morphology (McLean, 1988). Eight shell measurements were taken using Image J software (https://imagej.nih.gov/ij/) (Matabos *et al.*, 2008: fig. 1). A principal component analysis (PCA) was then performed on log-shape ratios after elimination of allometric changes, following Mosimann (1970) and Mosimann & James (1979). All variables were first log-transformed and 'size' for each individual was defined as the arithmetic mean of all variables. The log-shape ratio was then calculated by subtracting the log-size value from each variable for each individual.

RESULTS

From the 167 sequences analysed, a total of 72 haplotypes were identified across the seven *Lepetodrilus* species collected along the Northern and Eastern Pacific Ridges and revealed 186 segregating sites that included only two singletons and 183 parsimony-informative sites. Phylogenetic reconstructions highlighted seven main lineages including the *L. pustulosus* complex, *L. cristatus*, the *L. tevnianus* complex, two

northeastern Pacific clades including *L. gordensis* and *L. fucensis*, the Guaymas Basin species *L. guaymasensis* and, finally, the well-diversified *L. elevatus* complex (Fig. 2).

Lepetodrilus pustulosus was subdivided into two distinct lineages: *L. pustulosus* individuals from the EPR and the Galápagos Rift, and a southern lineage from the Pacific-Antarctic Ridge (31–38°S) previously highlighted by Johnson *et al*. (2008) (identified as *L.* aff. *pustulosus*). The former lineage included those individuals from 21°N to 17°S on the EPR and the Galápagos Rift, without genetic breaks across the whole EPR/Galápagos Rift ridge system. Similarly *L. cristatus* formed a single lineage with high genetic homogeneity along the whole EPR and the Pacific-Antarctic Ridge (21°N to 38°S).

The specimens attributed to the *L. tevnianus* complex displayed 78 segregating sites including five singletons, and four fixed nonsynonymous changes out of 82 mutations among all lineages. Both trees showed similar topology, with the occurrence of three distinct lineages highly supported by posterior probability (PP) and bootstrap (BS) values (Fig. 2). Individuals from the Galápagos Rift formed a lineage distinct from the EPR complex with an average divergence from the two EPR lineages of 12.3% and 11.9%, respectively (compared with 4.8% between the two EPR lineages). The calibration tree dated the vicariant event between *L. tevnianus* from the Galapagos Rift and the two other species from the EPR to around 50 Ma (CI 25.1–74.7 Ma) and the time of divergence between *L. tevnianus* and *L.* aff. *tevnianus* on the EPR to about 11 Ma (CI 3.6–17.8 Ma; Fig. 3).

Within the *L. elevatus/galriftensis* complex (77 sequences), 75 segregating sites including six singletons, and six nonsynonymous changes out of the 80 mutations were detected among all lineages. Both trees revealed the occurrence of four distinct clades or molecular taxonomic units (MOTUs) within the *L. e. elevatus/galriftensis* complex:

the *L. elevatus* northern clade (Clade 1; *L. elevatus s. s.* in Johnson *et al*., 2008), the *L. elevatus* southern clade (Clade 2; Matabos *et al*., 2008, and *L.* aff. *galriftensis* in Johnson *et al.*, 2008), *L.* aff. *elevatus* from the southern EPR and the Pacific-Antarctic Ridge (Clade 3) and *L. e. galriftensis* from the Galápagos Rift (Clade 4) (Fig. 2). None of the identified MOTUs shared any haplotypes. Within this diversified *L. elevatus* group, both trees displayed a similar topology, but BS values highlighted the difficulty of properly resolving the evolutionary history of this species complex using the available genetic data (Fig. 2). Both trees, however, suggest the occurrence of two vicariant events. The oldest one separated the southern (9°N–38°S) and northern (9–21°N EPR, Galápagos Rift) lineages, whereas the second produced the split of each clade into separate geographical units, the northern one giving rise to the monomorphic *L. e. galriftensis* species (Fig. 2). Under the stereomicroscope, Galápagos individuals were morphologically similar to *L. e. elevatus* on the EPR (Fig. 4), and we did not find any individual belonging to *L. e. elevatus* on the Galapagos Rift using the molecular-barcoding approach. Morphometric analyses confirmed the distinction between *L. e. galriftensis* from the Galápagos Rift and the two lineages of *L. e. elevatus* from the EPR (Fig. 5). The first axis of the PCA (48.1% of the total variance) segregated shells of the *L. e. elevatus* MOTUs from the EPR from the ones belonging to individuals collected on the Galapagos Rift, corresponding to *L. e. galriftensis* as described by McLean (1988) and the newly barcoded specimens used in the present study.

Kimura two-parameter genetic distances supported a more recent divergence between the two southern *L. elevatus* clades (i.e. *L.* aff. *elevatus* from the Pacific-Antarctic Ridge and the southern clade from 9°N to 21°S EPR) with 5.8% genetic divergence. *Lepetodrilus galriftensis* identified from the Galápagos Rift displayed among the highest genetic distances from the three other *L. elevatus* clades, ranging

from 7.4 to 8.6% (Table 3). A divergence of 8.1% between the northern and southern EPR *L. elevatus* clades dates the population split across the EPR to around 7 Ma (CI 5.9–8.5 Ma) (Fig. 3). Divergence within each clade arose at around 6 Ma (CI 4.5–7.6 Ma) for the northern *L. e. elevatus* and *L. e. galriftensis*, and 5.5 Ma (CI 3.9–7.2 Ma) for the southern *L e. elevatus* and *L. e. elevatus* from the Pacific-Antarctic Ridge (Fig. 3). Despite some differences, all splitting events within the complex seem to have occurred simultaneously between 7 and 5 Ma.

Lepetodrilus guaymasensis was distinct from the *L. elevatus/galriftensis* complex and formed a unique clade grouping all the specimens collected in the Guaymas Basin and the Costa Rica margin (Fig. 2). However, genetic divergences from the *L. elevatus/galriftensis* complex were very similar (7.5 to 9.6%) to those within the complex itself. These divergences are similar to that observed between the two sister species *L. fucensis* and *L. gordensis* separated by the Blanco Transform Fault Zone in the northeastern Pacific. Using the same time calibration, the divergence between *L. guaymasensis* and the *L. elevatus* species complex was estimated to occur *c*. 11.2 Ma (CI 11.0–11.9 Ma) (Fig. 3).

DISCUSSION

The genus *Lepetodrilus* was originally established to include seven distinct morphological species from the East Pacific ridges (i.e. Juan de Fuca Ridge, East Pacific Rise, Galapagos Rift and Guaymas Basin), including *L. elevatus* (with two subspecies, *L. e. elevatus* and *L. e. galriftensis*), *L. cristatus, L. pustulosus*, *L. ovalis*, *L. tevnianus* and *L. guaymasensis* on the EPR/Galápagos Rift, and *L. fucensis* in the northeastern Pacific (McLean, 1988, 1993). Molecular analyses revealed the presence of two divergent lineages along the northeastern Pacific system, subsequently subdivided

into two distinct species, *L. fucensis* and *L. gordensis*, with morphological differences between them (Johnson *et al.*, 2006). Along the EPR, cryptic lineages occur in at least three of the six morphological species (Johnson *et al.*, 2008; Plouviez *et al.*, 2009; Matabos *et al.*, 2011). The analysis of DNA sequences coding for mtCOI obtained from the Galapagos Rift revealed two additional lineages, i.e. for the *L. elevatus* and *L. tevnianus* complexes, for which no molecular data had been available to date. These new molecular data bring the number of genetically divergent lineages to 13 in the genus *Lepetodrilus* along the EPR/Guaymas and Galápagos ridge systems. The tree topologies suggest that *L. guaymasensis* diverged from the ancestor of *L. elevatus* before its subsequent and rapid radiation. The level of differentiation observed implies that the larval pelagic duration is not long enough to connect all vent sites of the EPR or that larval dispersal is quite often disrupted between one ridge segment and another.

Genetic patterns based on mtCOI sequences varied among taxa, with large-scale genetic homogeneity (*L. cristatus*), lack of structured populations with a high connectivity between the Galápagos Rift and EPR (*L. pustulosus*) and highly structured lineages with a geographical barrier between the EPR and the Galápagos Rift (*L. elevatus/galriftensis* and *L. tevnianus*). This wide range of distributional patterns may be related to differences in life-history traits, including reproduction and larval dispersal that affect species' ability to colonize distant territories, or diverging demographic histories with periods of extinctions and recolonization. Histological and anatomical analyses have shown a similar reproductive pattern among all species within the genus, characterized by continuous gametogenesis and pseudo-internal fertilization in the mantle cavity (Fretter, 1988; Warén & Bouchet, 2001; Tyler *et al.*, 2008), but their mode of larval development remains uncertain (Tyler *et al.*, 2008). Although earlier studies suggested phylogenetically-constrained planktonic lecithotrophic larvae (Berg,

1985; Eckelbarger, 1994), the maximum oocyte size in *L. elevatus* and *L. pustulosus* appeared more consistent with planktotrophic development (Tyler *et al.*, 2008). However, dispersal capabilities of lecithotrophic larvae are not fully understood and there is growing evidence that dispersal distance can be a poor determinant of species range size (Lester *et al.*, 2007).

Within the genus, the *L. elevatus* species complex appeared to be one of the most genetically structured species across its range, with four distinct lineages from 21°S/EPR to the Galápagos Rift. McLean (1988) originally described two morphologically distinct subspecies, namely *L. e. elevatus* and *L. e. galriftensis*, based on a difference in the height of the shell. Following this original description, several reports on *L. elevatus* revealed the presence of the two 'subspecies' in sympatry on the northern EPR at 9°50'N (Craddock *et al.*, 1997; Desbruyères, Segonzac & Bright, 2006). This finding was supported by genetic studies on these two distinct lineages along the EPR, although with one attributed to *L. e. galriftensis* (Craddock *et al.*, 1997; Johnson *et al.*, 2008), which led to an erroneous reported range for this subspecies. In this study, the addition of individuals from the Galápagos Rift has provided evidence that the two sister species found on the southern and northern parts of the EPR differ genetically and morphologically from *L. e. galriftensis* as originally described by McLean (1988). These results support the conclusion of a previous study, which reported that the two cryptic and hybridizing EPR species belong to *L. e. elevatus* (as opposed to *L. e. galriftensis*; Matabos *et al.*, 2008). The Galapagos Rift (90°W to 85.5°W) is separated from the EPR (at 102°W) by the presence of the 13,000 km² Galápagos microplate, the Hess Deep and the Galápagos Islands (Lonsdale, 1988). These features constitute strong, extant, geographical barriers between this segment of the Cocos-Nazca spreading centre and the EPR, preventing secondary contact between

the two divergent lineages. These barriers may explain why *L. e. galriftensis* is not observed over the whole EPR, despite the fact that its isolation time is probably too short to prevent local hybridization with the other lineages in sympatry. It would be interesting to explore intermediate segments lying on the other side of the Galapagos Islands, better to characterize the species' distribution in the area.

Lepetodrilus tevnianus also displayed strong genetic divergence (*c.* 12%) between the EPR and the Galápagos Rift; this is twice that of *L. e. elevatus/galriftensis* and three times that of the two other cryptic lineages already detected on the southern and northern EPR (Johnson *et al.*, 2008). This divergence confirms the role of the Galapagos Islands/Hess Deep as a physical barrier to dispersal, but the discrepancy in divergence between the two morphological species may be linked to differences in effective population sizes, generation time and habitat fragmentation. *Lepetodrilus elevatus* is a successful colonizer present in high numbers (thousands of individuals per sample), with a broad environmental niche (Mills, Mullineaux & Tyler, 2007; Matabos *et al.*, 2008), whereas *L. tevnianus* is a pioneer species present in low numbers and living almost exclusively in *Tevnia jerichonana* tubeworm bushes (Shank *et al.*, 1998; Mullineaux *et al.*, 2012). A lower effective population size of the former species due to the rarity of newly venting zones (diffuse venting habitats immediately following a eruptive/tectonic event are spatially less frequent) would result in reduced migration between vent fields and thus increase the probability of isolation. Strong variations in genetic distance between cryptic species have already been reported along the EPR for other gastropod taxa sharing a common geographical barrier (Matabos *et al.*, 2011)—due to the release of other barriers, population size variations, differing migration rates and strengths of selection against hybrids in secondary contact zones (Faure *et al.*, 2009; Plouviez *et al.*, 2013).

Within the *L. pustulosus* complex, no new divergent lineage was observed in the light of the additional samples from the Galápagos Rift, suggesting panmixia over the two ridge systems for this species. This result is surprising, considering the high level of genetic structure of the other species (this study; Johnson *et al.*, 2008; Matabos *et al.*, 2008, 2011; Plouviez *et al.*, 2009). Both *L. pustulosus* and *L. elevatus* appear to have similar reproductive features, with continuous gametogenesis and fertilization in the mantle cavity (Tyler *et al.*, 2008). They also produce similar types of larvae and display discontinuous recruitment (Mullineaux, Mills & Goldman, 1998). However, the difficulty of identifying larvae at the species level, along with the absence of data on the larval biology of *L. pustulosus* and *L. tevnianus*, make it difficult to understand the potential role of species' traits on the variations observed in genetic divergences (Adams *et al.*, 2010). Alternatively, this difference in species' ranges can be attributed to different demographic histories, global extinction of some lineages and the efficiency with which others recolonize new territories (Cunningham & Collins, 1998). *Lepetodrilus elevatus* is a highly competitive and successful species that can colonize several distinct habitats, from chimneys to mussel beds (Mills *et al.*, 2007; Matabos *et al.*, 2008). Conversely, *L. pustulosus* lives exclusively in *Riftia pachyptila* clumps (Mills *et al.*, 2007; personal observation); *R. pachyptila* also represents a single morphospecies without any genetic diversification (Coykendall *et al.*, 2011). We therefore hypothesize that other lineages of *L. pustulosus* may have gone extinct together with the assemblages of *R. pachyptila* at some specific locations during the isolation phase, 12 to 6 Ma, which generated the diversification of *L. elevatus*. The local extinction of *R. pachyptila* and *L. pustulosus* would have opened new niches that could then have been recolonized by the remaining populations following a recent demographic expansion. The last ridge reorganization that resulted in the present EPR

(Mammerickx, Herron & Dorman, 1980; Mammerickx & Klitgord, 1982) would have opened new pathways for this secondary introduction for the southern lineage. While this pathway would be available to the other species, in the case of the highly successful colonizer *L. elevatus*, the maintenance of divergent lineages might have created genetic barriers and thus slow down the recolonization process over the whole EPR. To this extent, the co-occurrence of divergent clades in sympatry within the *L. elevatus* complex most likely reflects ongoing secondary contacts. Lineage extinction is frequently mentioned in biogeographic studies to explain discrepancies in genetic patterns for species sharing a similar vicariant history (Cunningham & Collins, 1998).

Interestingly, *L. guaymasensis* also displays great genetic homogeneity over thousands of kilometers between the Guaymas Basin on the Sonora margin (27°35'N) and the Costa Rica margin (8°58'N). Both samples were collected in cold-seep habitats. The colonization of seeps by this species was probably facilitated by the close proximity of vents and seeps (less than 60 km apart) in the Guaymas Basin, where these two connected habitats share a number of species (Portail *et al.*, 2015). In contrast to the discontinuous system of ridge segments typifying the northern EPR/Guaymas basin, the subduction trench of the Cocos-Nazca spreading centre may represent a more efficient pathway for subsequent stepwise southward migration of the species along the continental slope, particularly if seeps are more widespread and continuous than previously known.

In order to date the tectonic events that produced population separation, we calibrated genetic data according to the same geological events proposed by Johnson *et al.* (2006) (i.e. the progressive subduction of the Farallon plate from 29 to 25 Ma, and the formation of the Blanco Transform Fault Zone and the Cascadia Depression about 5 Ma) and the separation of the Guaymas Basin 12.5 to 11 Ma (Mammerickx & Klitgord,

1982). In this study, we hypothesized that the subduction of the Farallon plate under the North American plate corresponds to the vicariant event resulting in the speciation of *L. gordensis* and *L. guaymasensis*, as revealed by the present phylogenetic reconstruction. This calibration date indicates that the population-splitting events within the *L. elevatus* complex occurred over a relatively short interval (from 7 to 5 Ma). The EPR has a complex but well-studied tectonic history, which can shed light on the mechanisms behind the various genetic divergences observed. The EPR underwent three major reorganizations during the last 25 Ma: (1) the breaking of the Farallon plate and the opening of the Nazca-Cocos spreading centre (which includes the Galápagos Rift) around 22 Ma; (2) the opening of the ancestral EPR between 11 and 12.5 Ma and (3) the extinction of a number of spreading segments, leaving the EPR as the only active spreading center after 6.5 Ma (Mammerickx & Klitgord, 1982; Lonsdale, 2005) (Fig. 6). The split of the Farallon plate (Fig. 6A, C) induced major changes in the region, including the acceleration and reorientation/rotation of spreading axes on the EPR and the formation of a number of risecrest microplates (e.g. Bauer and Mendoza microplates; Eakins & Lonsdale, 2003) (Fig. 6B, D, F). Most divergences observed among lineages from the EPR and Galápagos Rift appear to correspond to the major reorganizations that occurred between 12.5 and 6.5 Ma.

After the Middle Miocene plate reorganization (12.5 to 11 Ma), a whole segment of the Pacific Cocos spreading centre died between 29°30'N and 23°30'N, by either subduction or as abandoned spreading centres (Mammerickx & Klitgord, 1982). This history provides strong support for the initial isolation of *L. guaymasensis* occurring 11 to 13 Ma on a segment that did not reconnect to the current EPR. At the same time, a new spreading centre developed south of Baja California (the ancestral EPR), while the older spreading centre, including the Mathematician Ridge, remained

active in the west between 17°N and 10°N for a short time after this major reorganization (Fig. 6D). In the southern EPR, affected by the same major ridge reorganization, an active spreading centre (i.e. the Galápagos Rise; Mammerickx *et al.*, 1980) remained west of the ancestral EPR until 6.5 Ma, creating the large Bauer microplate at 10–15°S (Fig. 6D, F; 18.2 to 6.5 Ma). The extinction of active segments such as the Mathematician Ridge or the Galápagos Rise west of the active EPR 6.5 Ma may have quasi-simultaneously isolated the four *L. elevatus* lineages, including Clades 1 to 3 on the EPR and *L. e. galriftensis* (i.e. Clade 4) from the Galápagos Rift, on distinct spreading centres. Together with the formation of the Easter microplate 5–6 Ma, the appearance of a number of microplates may have enhanced isolation and resulted in vicariant events on either side of these risecrest features (Fig. 6B, D, F). Previous studies have already pointed out the role of the Bauer microplate, existing from 17 to 6 Ma between 10°S and 15°S (Eakins & Lonsdale, 2003), or the shift and extinction of the Mathematician Ridge from 12 to 6.5 Ma at 10°N (Mammerickx & Klitgord, 1982), in the separation of *L. e. elevatus* Clade 1 and Clade 2 (Matabos *et al.*, 2008; Plouviez *et al.*, 2009). About 6 Ma, further south at around 25°S, the ridge was offset in at least two places where the current Easter microplate (Naar & Hey, 1991) is located. This feature corroborates the present distribution of the southern lineage of *L. e. elevatus* Clade 3, as well as the separation of other vent species such as crabs, vent mussels and vestimentiferan tubeworms (Guinot & Hurtado, 2003; Won *et al.*, 2003; Hurtado *et al.*, 2004). The finalization of the Easter microplate less than 2 Ma may have opened a new passage along its flanks, as demonstrated by the presence of some Pacific–Antarctic Ridge species at 21°33'S (Matabos *et al.*, 2011) and a hybrid zone for vent mussels at 23°S (Johnson *et al.*, 2013). However, the formation of Pito Deep on its eastern side still remains a semipermeable barrier, limiting northward migration for Pacific–

Antarctic Ridge species (Naar *et al.*, 1991). In the case of *L. elevatus* Clade 3, the barrier associated with the Easter microplate seems to have opened somewhat, because Johnson *et al*. (2008) reported the presence of *L. elevatus* Clade 3 up to 7°S. The absence of sampling locations of available sequences in GenBank, however, did not allow us to confirm this clade beyond 21°S.

Although the use of molecular phylogenetic techniques has increased our capacity to describe the current vent biodiversity, one concern is our ability morphologically to identify cryptic species in samples. Diagnosis of a species traditionally requires morphological or other criteria, (but see Johnson *et al.* , 2015 for the use of sequence data as a new criterion using a barcode approach). From the analyses of a high number of individuals sampled in mussel beds and *R. pachyptila* clumps along the 5,000-km stretch of the EPR, it is obvious that the sister species to *L. elevatus s. s.* shows plasticity in its shell elevation, varying with the type of habitat occupied. For example, individuals from the *L. elevatus* Clade 2 were only found in mussel beds (personal observation). With this observation in mind, the original diagnostic feature (i.e. shell height) proposed by McLean (1988) to segregate *L. e. elevatus* from *L. e. galriftensis* appears unjustified in the light of our analyses of tens of thousands of individuals. Even if the ratio between shell height and length appears to separate *L. e. elevatus* and *L. e. galriftensis*, the observed continuum of shell height and the overlap of some individuals along the first PCA axis highlights the difficulty of clearly discriminating these two subspecies based on shell morphology (Figs 4, 5). In the absence of sequencing, knowing the sampling location can be helpful to assign individuals to a given clade, but in the transition regions between the southern and northern EPR, or beyond 21°S, there is currently no available diagnostic trait to segregate Clade 1 from Clade 2, or Clade 2 from Clade 3.

Therefore, despite the species-level divergences observed (Peek *et al.*, 1997), and until clear morphological diagnostic criteria can be identified among the four *L. elevatus* cryptic species, we propose to redefine the *L. elevatus* complex as a single species that includes four genetically distinct lineages. In addition, the fact that Clades 1 and 2 co-exist and hybridize at 9°50'N (Matabos *et al.*, 2008) rules out the possibility of erecting these MOTUs as 'true' distinct species. Following the recommendations of Samadi & Barberousse (2006), the existence of fertile hybridization indeed questions the so-called species status of the species within the complex. Coupled with the fact that divergences between the four cryptic mitochondrial lineages of the *L. elevatus* complex are nearly identical, we therefore recommend keeping the original name *L. elevatus* for these 'geographic' MOTUs along the EPR/Galápagos ridge systems in ecological studies, to avoid misidentification in the absence of barcoding. Understanding the demographic and evolutionary history of the divergent lineages requires a multilocus approach, because different genes tell different stories for species experiencing ongoing speciation, but also provide additional information on the putative extinction/recolonization processes.

ACKNOWLEDGEMENTS

The authors would like to thank the captain and crew of R/V *L'Atalante* and the pilots of the human-operated vehicle *Nautile*. We are also grateful to the chief scientists Leigh Marsh (NOC) and Nicole Raineault (Ocean Exploration Trust) who led the Nautilus 2015 cruise on the Galápagos Rift, and Stéphane Hourdez and Chuck Fisher for their assistance in providing the samples. We thank Anne Godfroy, chief scientist of the 2010 BIG cruise, and Marie Portail for samples from the Guaymas Basin. Finally, we would like to thank two anonymous reviewers and Yasunori Kano for their comments on a

previous version of the manuscript. This work was supported by the ‘Laboratoire d'Excellence’ LabexMER (ANR-10-LABX-19) and co-funded by a grant from the French government under the ‘Investissements d'Avenir’ investment expenditure program.

REFERENCES

ADAMS, D.K., MILLS, S.W., SHANK, T.M. & MULLINEAUX, L.S. 2010. Expanding dispersal studies at hydrothermal vents through species identification of cryptic larval forms. *Marine Biology*, **157**: 1049–1062.

BACHRATY, C., LEGENDRE, P. & DESBRUYÈRES, D. 2009. Biogeographic relationships among deep-sea hydrothermal vent faunas at global scale. *Deep-Sea Research Part I*, **56**: 1371–1378.

BERG, C.J. 1985. Reproductive strategies of mollusks from abyssal hydrothermal vent communities. *Bulletin of the Biological Society of Washington*, **6**: 185–197.

COYKENDALL, D.K., JOHNSON, S.B., KARL, S. A, LUTZ, R.A. & VRIJENHOEK, R.C. 2011. Genetic diversity and demographic instability in *Riftia pachyptila* tubeworms from eastern Pacific hydrothermal vents. *BMC Evolutionary Biology*, **11**: 96.

CRADDOCK, C., LUTZ, R.A. & VRIJENHOEK, R.C. 1997. Patterns of dispersal and larval development of archaeogastropod limpets at hydrothermal vents in the eastern Pacific. *Journal of Experimental Marine Biology and Ecology*, **210**: 37–51.

CUNNINGHAM, C.W. & COLLINS, T.M. 1998. Beyond area relationships: extinction and recolonization in molecular marine biogeography. In: *Molecular approaches*

to ecology and evolution (R. DeSalle & B. Schierwater, eds), pp. 297–321. Birkhauser Verlag, Basel.

DEREEPER, A., GUIGNON, V., BLANC, G., AUDIC, S., BUFFET, S., CHEVENET, F., DUFAYARD, J.F., GUINDON, S., LEFORT, V., LESCOT, M., CLAVERIE, J.M. & GASCUEL, O. 2008. Phylogeny.fr: robust phylogenetic analysis for the non-specialist. *Nucleic Acids Research*, **36**: W465-9.

DESBRUYÈRES, D., SEGONZAC, M. & BRIGHT, M. 2006. Handbook of deep-sea hydrothermal vent fauna. Second completely revised edition. *Denisia*, **18**: 1–544.

DOYLE, J.J. & DOYLE, J.L. 1987. A rapid DNA isolation procedure for small quantities of fresh leaf tissue. *Phytochemical Bulletin*, **19**: 11–15.

EAKINS, B.W. & LONSDALE, P.F. 2003. Structural patterns and tectonic history of the Bauer microplate, Eastern Tropical Pacific. *Marine Geophysical Researches*, **24**: 171–205.

ECKELBARGER, K.J. 1994. Diversity of metazoan ovaries and vitellogenic mechanisms—implications for life history theory. *Proceedings of the Biological Society of Washington*, **107**: 193–218.

FAURE, B., JOLLIVET, D., TANGUY, A., BONHOMME, F. & BIERNE, N. 2009. Speciation in the deep sea: multi-locus analysis of divergence and gene flow between two hybridizing species of hydrothermal vent mussels. *PLoS One*, **4**: e6485.

FOLMER, O., BLACK, M., HOEH, W., LUTZ, R.A. & VRIJENHOEK, R. 1994. DNA primers for amplification of mitochondrial cytochrome *c* oxidase subunit I from diverse metazoan invertebrates. *Molecular Marine Biology and Biotechnology*,

3: 294–299.

FRETTER, V. 1988. New archaeogastropod limpets from hydrothermal vents; superfamily Lepetodrilacea II. Anatomy. *Philosophical Transactions of the Royal Society of London. Series B, Biological Sciences*, **319**: 33–82.

GUINOT, D. & HURTADO, L.A. 2003. Two new species of hydrothermal vent crabs of the genus *Bythograea* from the southern East Pacific Rise and from the Galapagos Rift (Crustacea Decapoda Brachyura Bythograeidae). *Comptes Rendus Biologies*, **326**: 423–439.

HANNINGTON, M.D., JONASSON, I.R., HERZIG, P.M. & PETERSEN, S. 1995. Physical and chemical processes of seafloor mineralization at mid-ocean ridges. *Geophysical Monographs*, **91**: 115–157.

HENDRY, A.P., LOHMANN, L.G., CONTI, E., CRACRAFT, J., CRANDALL, K.A., FAITH, D.P., HÄUSER, C., JOLY, C.A., KOGURE, K., LARIGAUDERIE, A., MAGALLÓN, S., MORITZ, C., TILLIER, S., ZARDOYA, R., PRIEUR-RICHARD, A.H., WALTHER, B.A., YAHARA, T. & DONOGHUE, M.J. 2010. Evolutionary biology in biodiversity science, conservation, and policy: a call to action. *Evolution*, **64**: 1517–1528.

HURTADO, L.A., LUTZ, R.A. & VRIJENHOEK, R.C. 2004. Distinct patterns of genetic differentiation among annelids of eastern Pacific hydrothermal vents. *Molecular Ecology*, **13**: 2603–2615.

JOHNSON, S.B., WARÉN, A., TUNNICLIFFE, V., VAN DOVER, C., WHEAT, C.G., SCHULTZ, T.F. & VRIJENHOEK, R.C. 2015. Molecular taxonomy and naming of five cryptic species of *Alviniconcha* snails (Gastropoda: Abyssochrysoidea) from hydrothermal vents. *Systematics and Biodiversity*, **13**:

278–295.

JOHNSON, S.B., WARÉN, A. & VRIJENHOEK, R.C. 2008. DNA Barcoding of *Lepetodrilus* limpets reveals cryptic species. *Journal of Shellfish Research*, **27**: 43–51.

JOHNSON, S.B., WON, Y.-J., HARVEY, J.B. & VRIJENHOEK, R.C. 2013. A hybrid zone between *Bathymodiolus* mussel lineages from eastern Pacific hydrothermal vents. *BMC Evolutionary Biology*, **13**: 21.

JOHNSON, S.B., YOUNG, C.R., JONES, W.J., WARÉN, A. & VRIJENHOEK, R.C. 2006. Migration, isolation, and speciation of hydrothermal vent limpets (Gastropoda; Lepetodrilidae) across the Blanco transform fault. *Biological Bulletin*, **210**: 140–157.

JOLLIVET, D., CHEVALDONNÉ, P. & PLANQUE, B. 1999. Hydrothermal-vent alvinellid polychaete dispersal in the eastern Pacific. 2. A metapopulation model based on habitat shifts. *Evolution*, **53**: 1128–1142.

JOLLY, M., VIARD, F., WEINMAYR, G., GENTIL, F., THIÉBAUT, E. & JOLLIVET, D. 2003. Does the genetic structure of *Pectinaria koreni* (Polychaeta: Pectinariidae) conform to a source-sink metapopulation model at the scale of the Baie de Seine? *Helgoland Marine Research*, **56**: 238–246.

KIMURA, M. 1980. A simple method for estimating evolutionary rates of base substitutions through comparative studies of nucleotide sequences. *Journal of Molecular Evolution*, **15**: 111–120.

LESTER, S.E., RUTTENBERG, B.I., GAINES, S.D. & KINLAN, B.P. 2007. The relationship between dispersal ability and geographic range size. *Ecology Letters*, **10**: 745–758.

LONSDALE, P.F. 1988. Structural pattern of the Galápagos microplate and evolution of the Galápagos triple junctions. *Journal of Geophysical Research*, **93**: 13551–13574.

LONSDALE, P. 2005. Creation of the Cocos and Nazca plates by fission of the Farallon plate. *Tectonophysics*, **404**: 237–264.

MAMMERICKX, J., HERRON, E. & DORMAN, L. 1980. Evidence for two fossil spreading ridges in the southeast Pacific. *Geological Society of America Bulletin*, **91**: 263–271.

MAMMERICKX, J. & KLITGORD, K.D. 1982. Northern East Pacific Rise: evolution from 25 m.y. B.P. to the present. *Journal of Geophysical Research*, **87**: 6751–6759.

MARCUS, J., TUNNICLIFFE, V. & BUTTERFIELD, D.A. 2009. Post-eruption succession of macrofaunal communities at diffuse flow hydrothermal vents on Axial Volcano, Juan de Fuca Ridge, Northeast Pacific. *Deep Sea Research Part II: Topical Studies in Oceanography*, **56**: 1586–1598.

MARSH, A.G., MULLINEAUX, L.S., YOUNG, C.M. & MANAHAN, D.T. 2001. Larval dispersal potential of the tubeworm *Riftia pachyptila* at deep-sea hydrothermal vents. *Nature*, **411**: 77–80.

MATABOS, M., PLOUVIEZ, S., HOURDEZ, S., DESBRUYÈRES, D., LEGENDRE, P., WARÉN, A., JOLLIVET, D. & THIÉBAUT, E. 2011. Faunal changes and geographic crypticism indicate the occurrence of a biogeographic transition zone along the southern East Pacific Rise. *Journal of Biogeography*, **38**: 575–594.

MATABOS, M., THIÉBAUT, E., LE GUEN, D., SADOSKY, F., JOLLIVET, D. & BONHOMME, F. 2008. Geographic clines and stepping-stone patterns detected

along the East Pacific Rise in the vetigastropod *Lepetodrilus elevatus* reflect species crypticism. *Marine Biology*, **153**: 545–563.

MCGILLICUDDY, D.J., LAVELLE, J.W., THURNHERR, A.M., KOSNYREV, V.K. & MULLINEAUX, L.S. 2010. Larval dispersion along an axially symmetric mid-ocean ridge. *Deep Sea Research Part I: Oceanographic Research Papers*, **57**: 880–892.

MCLEAN, J.H. 1988. New archaeogastropod limpets from hydrothermal vents: Superfamily Lepetodrolacea: I. Systematic descriptions. *Philosophical Transactions of the Royal Society of London. Series B, Biological Sciences*, **319**: 1–32.

MCLEAN, J.H. 1993. New species and records of *Lepetodrilus* (Vetigastropoda: Lepetodrilidae) from hydrothermal vents. *Veliger*, **36**: 27–35.

MILLS, S.W., MULLINEAUX, L.S. & TYLER, P.A. 2007. Habitat associations in gastropod species at East Pacific Rise hydrothermal vents (9 degrees 50'N). *Biological Bulletin*, **212**: 185–194.

MOSIMANN, J. & JAMES, F. 1979. New statistical methods for allometry with application to Florida red-winged blackbirds. *Evolution*, **33**: 444–459.

MOSIMANN, J.E. 1970. Size allometry: size and shape variables with characterizations of the lognormal and generalized gamma distributions. *Journal of the American Statistical Association*, **65**: 930–945.

MULLINEAUX, L.S., ADAMS, D.K., MILLS, S.W. & BEAULIEU, S.E. 2010. Larvae from afar colonize deep-sea hydrothermal vents after a catastrophic eruption. *Proceedings of the National Academy of Sciences of the USA*, **107**: 7829–7834.

MULLINEAUX, L.S., LE BRIS, N., MILLS, S.W., HENRI, P., BAYER, S.R., SECRIST, R.G. & SIU, N. 2012. Detecting the influence of initial pioneers on succession at deep-sea vents. *PLoS One*, **7**: e50015.

MULLINEAUX, L.S., MILLS, S.W. & GOLDMAN, E. 1998. Recruitment variation during a pilot colonization study of hydrothermal vents (9°50'N, East Pacific Rise). *Deep-Sea Research Part II: Topical Studies in Oceanography*, **45**: 441–464.

MULLINEAUX, L.S., SPEER, K.G., THURNHERR, A.M., MALTRUD, M.E. & VANGRIESHEIM, A. 2002. Implications of cross-axis flow for larval dispersal along mid-ocean ridges. *Cahiers de Biologie Marine*, **43**: 281–284.

NAAR, D.F. & HEY, R.N. 1991. Tectonic evolution of the Easter Microplate. *Journal of Geophysical Research*, **96**: 7961–7993.

NAAR, D.F., MARTINEZ, F., HEY, R.N., REED IV, T.B. & STEIN, S. 1991. Pito Rift: how a large-offset rift propagates. *Marine Geophysical Researches*, **13**: 287–309.

PEEK, A.S., GUSTAFSON, R.G., LUTZ, R.A. & VRIJENHOEK, R.C. 1997. Evolutionary relationships of deep-sea hydrothermal vent and cold-water seep clams (Bivalvia: Vesicomyidae): results from the mitochondrial cytochrome oxidase subunit I. *Marine Biology*, **130**: 151–161.

PLOUVIEZ, S., FAURE, B., LE GUEN, D., LALLIER, F.H., BIERNE, N. & JOLLIVET, D. 2013. A new barrier to dispersal trapped old genetic clines that escaped the Easter microplate tension zone of the Pacific vent mussels. *PLoS One*, **8**: e81555.

PLOUVIEZ, S., SHANK, T.M., FAURE, B., DAGUIN-THIÉBAUT, C., VIARD, F.,

LALLIER, F.H. & JOLLIVET, D. 2009. Comparative phylogeography among hydrothermal vent species along the East Pacific Rise reveals vicariant processes and population expansion in the south. *Molecular Ecology*, **18**: 3903–3917.

PORTAIL, M., OLU, K., ESCOBAR-BRIONES, E., CAPRAIS, J.C., MENOT, L., WAELES, M., CRUAUD, P., SARRADIN, P., GODFROY, A. & SARRAZIN, J. 2015. Comparative study of vent and seep macrofaunal communities in the Guaymas Basin. *Biogeosciences*, **12**: 5455–5479.

POSADA, D. & CRANDALL, K.A. 1998. MODELTEST: testing the model of DNA substitution. *Bioinformatics*, **14**: 817–818.

RONQUIST, F. & HUELSENBECK, J.P. 2003. MrBayes 3: Bayesian phylogenetic inference under mixed models. *Bioinformatics*, **19**: 1572–1574.

SAMADI, S. & BARBEROUSSE, A. 2006. The tree, the network, and the species. *Biological Journal of the Linnean Society*, **89**: 509–521.

SHANK, T.M., FORNARI, D.J., VON DAMM, K.L., LILLEY, M.D., HAYMON, R.M. & LUTZ, R.A. 1998. Temporal and spatial patterns of biological community development at nascent deep-sea hydrothermal vents (9°50′ N, East Pacific Rise). *Deep-Sea Research Part II: Topical Studies in Oceanography*, **45**: 465–515.

TAMURA, K., STECHER, G., PETERSON, D., FILIPSKI, A. & KUMAR, S. 2013. MEGA6: Molecular Evolutionary Genetics Analysis version 6.0. *Molecular Biology and Evolution*, **30**: 2725–2729.

TUNNICLIFFE, V. 1988. Biogeography and evolution of hydrothermal-vent fauna in the eastern Pacific Ocean. *Proceedings of the Royal Society B: Biological Sciences*, **233**: 347–366.

TUNNICLIFFE, V. & FOWLER, C.M.R. 1996. Influence of sea-floor spreading on the global hydrothermal vent fauna. *Nature*, **379**: 531–533.

TYLER, P.A., PENDLEBURY, S., MILLS, S.W., MULLINEAUX, L., ECKELBARGER, K.J., BAKER, M. & YOUNG, C.M. 2008. Reproduction of gastropods from vents on the East Pacific rise and the mid-Atlantic ridge. *Journal of Shellfish Research*, **27**: 107–118.

VRIJENHOEK, R.C. 1997. Gene flow and genetic diversity in naturally fragmented metapopulations of deep-sea hydrothermal vent animals. *Journal of Heredity*, **88**: 285–293.

VRIJENHOEK, R.C. 2010. Genetic diversity and connectivity of deep-sea hydrothermal vent metapopulations. *Molecular Ecology*, **19**: 4391–411.

WARÉN, A. & BOUCHET, P. 2001. Gastropoda and Monoplacophora from hydrothermal vents and seeps: new taxa and records. *Veliger*, **44**: 116–231.

WATREMEZ, P. & KERVEVAN, C. 1990. Origine des variations de l'activité hydrothermale: premiers éléments de réponse d'un modèle numérique simple. *Compte Rendus de l'Académie des Sciences de Paris, Série II*, **311**: 153–158.

WON, Y., YOUNG, C.R., LUTZ, R.A. & VRIJENHOEK, R.C. 2003. Dispersal barriers and isolation among deep-sea mussel populations (Mytilidae: *Bathymodiolus*) from eastern Pacific hydrothermal vents. *Molecular Ecology*, **12**: 169–184.

Figure captions

Figure 1. Map of the East Pacific ridge systems. Stars represent sampling localities. Abbreviations: CRM, Costa Rica margin; NE Pacific, northeastern Pacific ridge system made up of Explorer (E), Juan de Fuca (JdF) and Gorda (G) ridges; SM, Sonora margin.

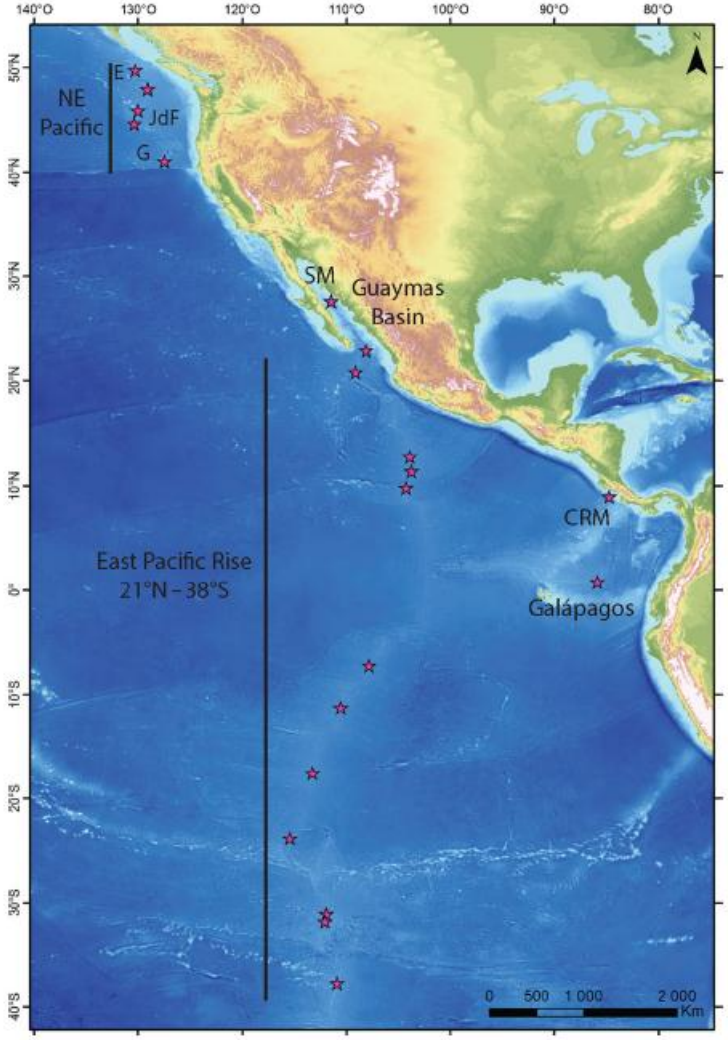

Figure 2. Bayesian tree based on unique mtCOI haplotypes from 72 *Lepetodrilus* and 1 *Gorgoleptis spiralis* samples following the Hasegawa, Kishino and Yano model (HKY+G+I). Numbers next to nodes correspond to Bayesian PP (above node) and BS values based on 100 resampling of dataset (below node). Blue brackets highlight the seven species complexes (see Results). See Tables 1 and 2 for details of sequences used and geographical locations. Abbreviations: EPR, East Pacific Rise; GAL, Galápagos; JdF, Juan de Fuca Ridge.

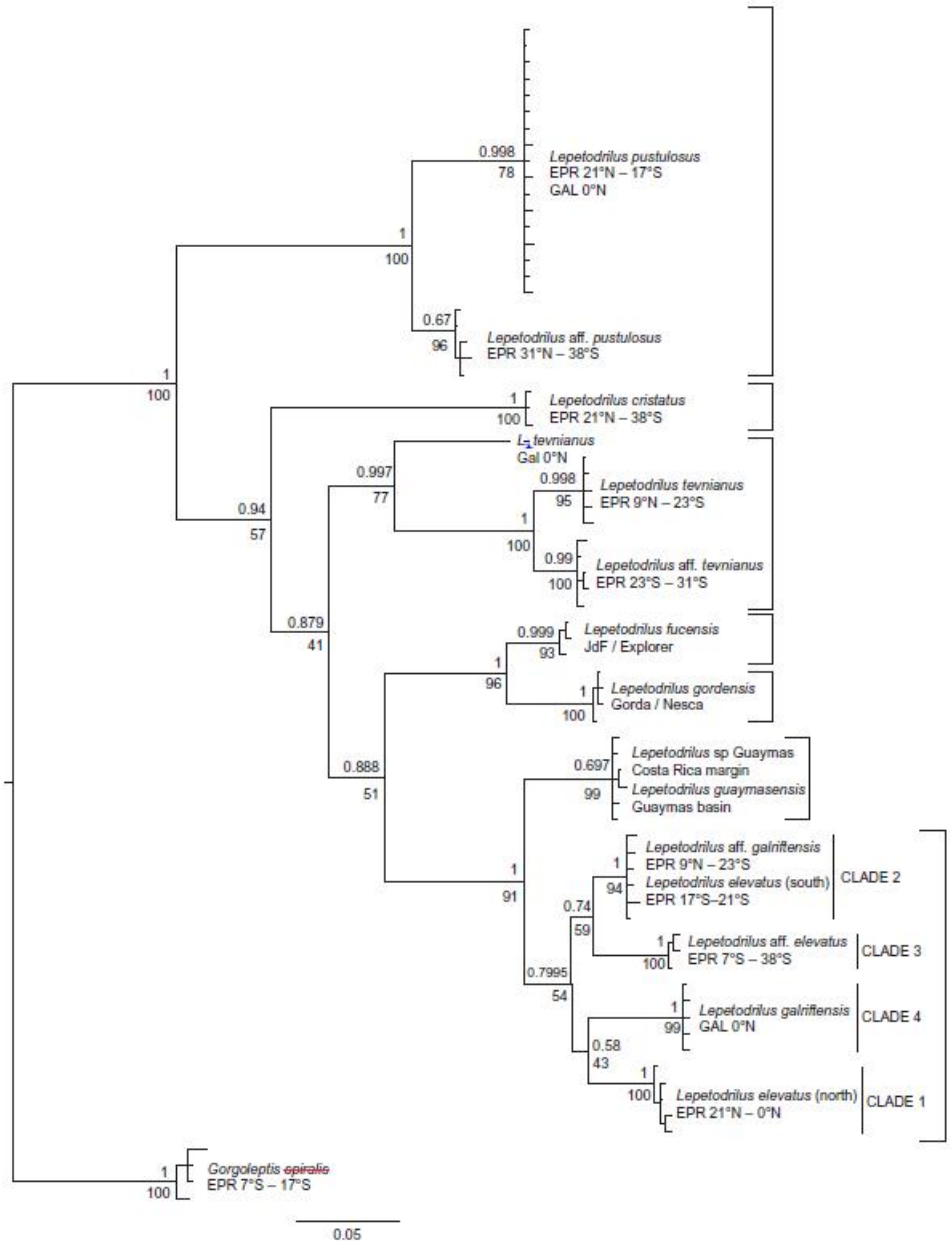

Figure 3. Time calibration (using the RelTime method in Mega v. 7.0) computed on the BI tree based on unique mtCOI haplotypes from the 72 *Lepetodrilus* and 1 *Gorgoleptis spiralis* samples following Hasegawa, Kishino and Yano model (HKY+G+I). Numbers next to nodes correspond to the time since divergence (Ma); white bars indicate 95% CI. See Table 1 for details of sequences used and geographical locations.

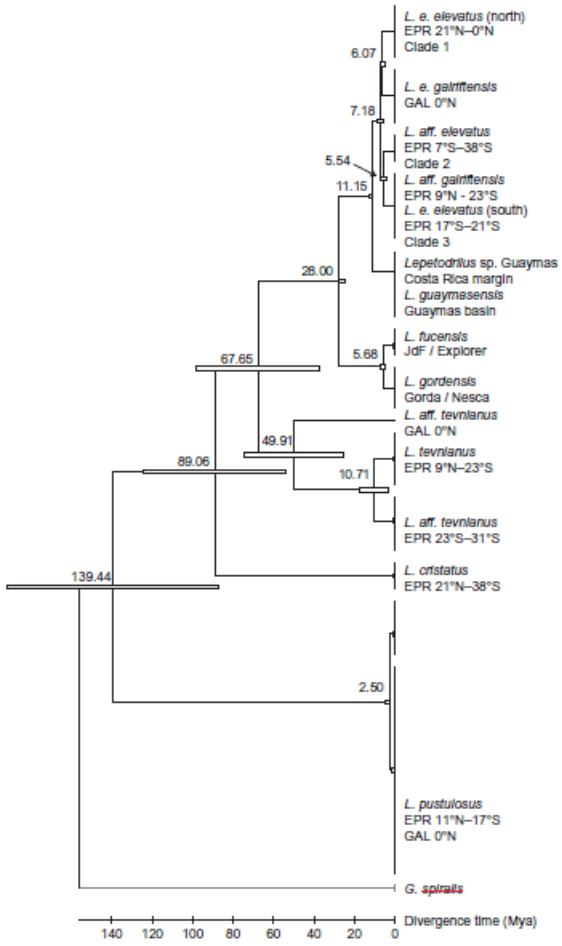

Figure 4. A–D. Photographs of *Lepetodrilus* species from the Galápagos Rift. **A, B.** Dorsal and ventral views of *L. elevatus galriftensis*. **C.** *L. pustulosus*. **D.** *L. tevnianus*. **E, F.** Lateral and dorsal views of *L. guaymasensis* from Sonora margin in Guaymas Basin. Scale bars = 1 mm.

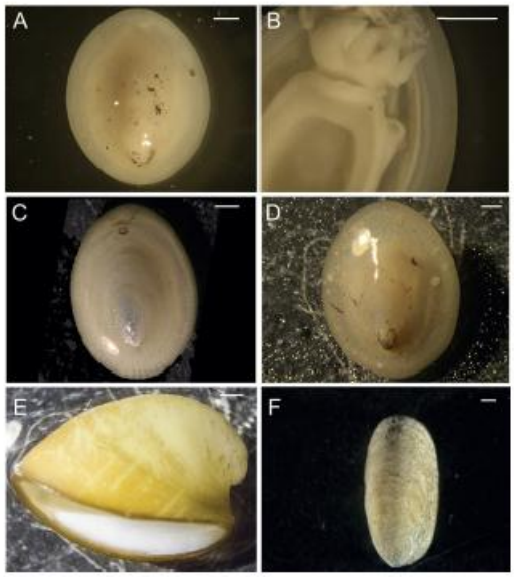

Figure 5. PCA on morphometric data for individuals of *Lepetodrilus elevatus galriftensis* and *L. e. elevatus* from East Pacific Rise and Galápagos Rift. *L. e. elevatus* 'north' correspond to individuals from Clade 1 and 'south' from Clade 2. 'Shells' are empty shells from the Galápagos morphologically identified as *L. e. galriftensis* (LACM 2528). Abbreviations: H, shell height (greatest vertical distance from apex to plane of aperture); L1, anterior length (anterior edge of shell to apex); L2, posterior length (posterior edge of shell to apex); Lbas, basal length (length of aperture); Lcurv, curvilinear shell length (total length from anterior edge to lip of protoconch); Lob, oblique length (maximal distance from anterior edge to posterior part of shell); Ltot, total shell length (greatest distance between posterior and anterior ends); W, shell width (greatest distance perpendicular to anteroposterior axis). See Matabos *et al.* (2008: fig. 1) for details on measurements.

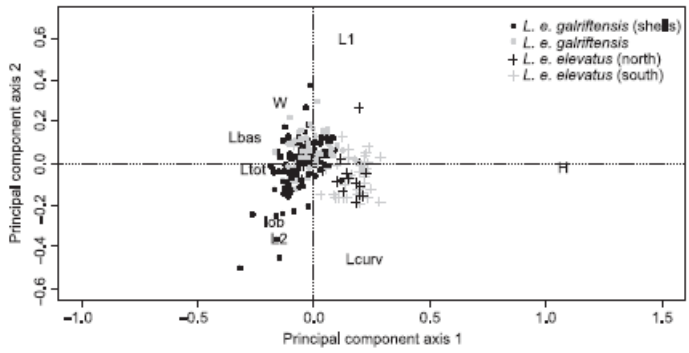

Figure 6. Schematic view of East Pacific Rise formation since Late Miocene (25 Ma) until today, showing tectonic features that might have affected distribution of *Lepetodrilus* populations. All figures were redrawn after Mammerickx *et al*. (1980) and Mammerickx & Klitford (1982). **A, B.** 12.5–11 Ma **(A)** and 6.5 Ma **(B)** reorganizations in northern EPR with abandoned ridges in grey dashed lines. **C–E.** Schematic evolution of the whole EPR from 25 Ma to present. Line with crosses: abandoned spreading centre separating the Guaymas basin. **F.** Evolution of Bauer microplate in southern EPR from 23 Ma to present. Black lines represent active ridge segments; rows of black dots represent abandoned ridge segments; grey dashed lines represent fracture zones; hatched areas represent active microplates. Abbreviations for ancient tectonic features: Ma, Mathematician Ridge; R, Rivera plate; G, Gallego Rise; M, Mendoza Rise; R, Roggeveen Rise; S, Selkirk Rise; G.R., Galápagos Rise. Split of Farallon plate opened Guadalupe-Nazca spreading centre that includes Galápagos Rift and generated emergence of a number of microplates in the south, including Bauer plate. This microplate lasted until Late Miocene reorganization **(E, F).** Opening of ancestral EPR during Middle Miocene reorganization, 12.5–11 Ma, also produced several microplates in the north **(B, D).** Extinctions of active segments such as Mathematician Ridge (M) or Galápagos Rise (G) during Late Miocene reorganization initiated 6.5 Ma might have simultaneously isolated the four lineages along EPR (**B, E, F**). Since Late Miocene reorganization, the current EPR remains the only active ridge, with opening of new pathways for the previously-separated lineages **(E, F).**

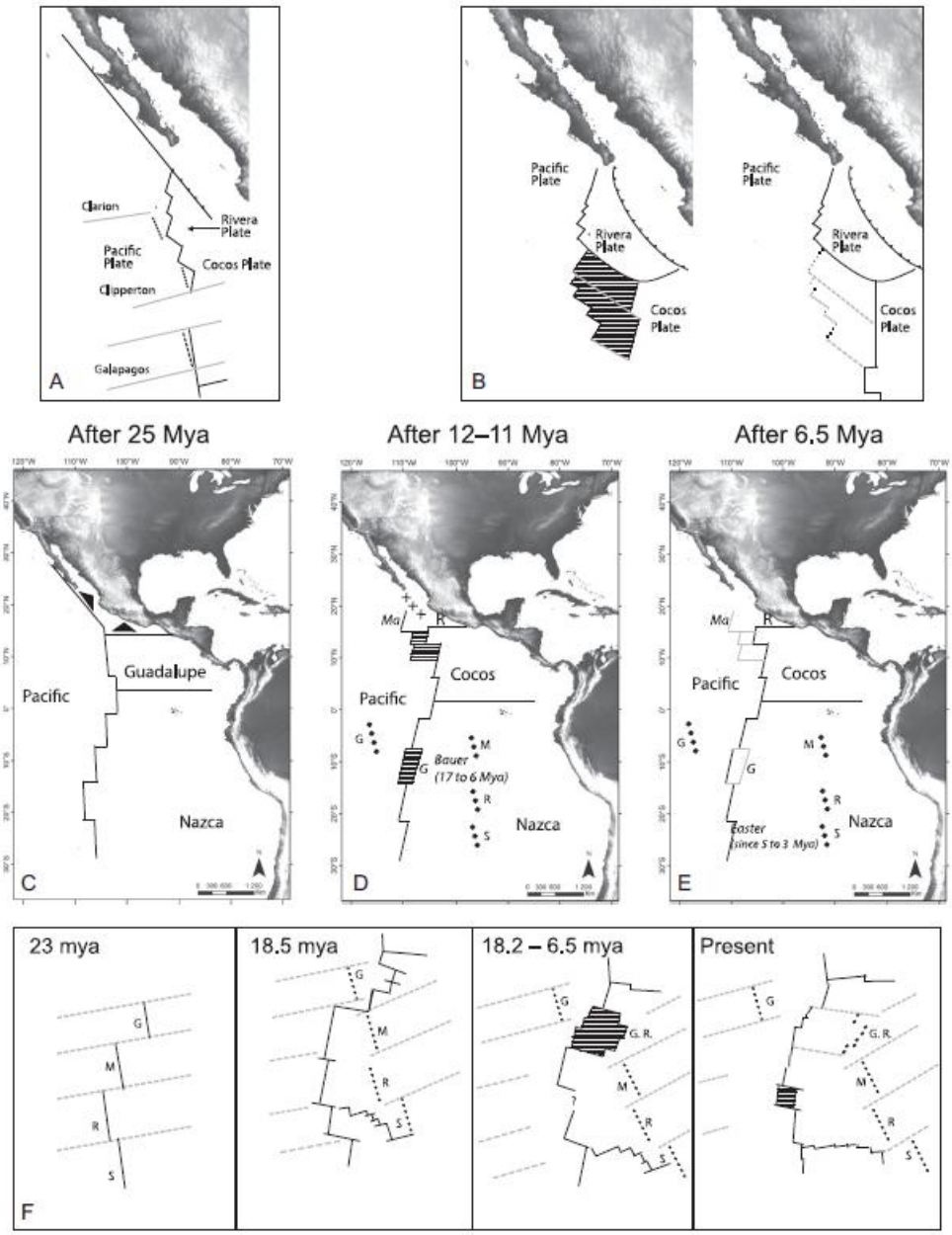
Clarion
Rivera Plate
Pacific Plate
Cocos Plate
Clipperton
Galapagos
A
Pacific Plate
Rivera Plate
Cocos Plate
B
After 25 Mya
Guadalupe
Pacific
Nazca
C
After 12–11 Mya
Ma
R
Cocos
Pacific
G
M
Bauer (17 to 6 Mya)
R
S
Nazca
D
After 6.5 Mya
Ma
R
Cocos
Pacific
G
M
G
R
S
Easter (since 5 to 3 Mya)
Nazca
E
23 mya
G
M
R
S
F
18.5 mya
G
M
R
S
18.2 – 6.5 mya
G
G. R.
M
R
S
Present
G
G. R.
M
R
S

Table 1. Species and localities of *Lepetodrilus pustulosus*, *L. tevnianus* and *L. e. galriftensis* individuals from the Galápagos Rift and *L. guaymasensis* from the Guaymas Basin. Abbreviation: *N*, number of individuals used for sequencing of portion of mtCOI gene.

Species	Location	Station	Museum voucher	Latitude	Longitude	Dive	*N*
Lepetodrilus pustulosus	Galápagos	NA063-009	MCZ383295	0°46.174'N	85°54.698'W	H1432	15
	Galápagos	NA063-023	MCZ383300	0°46.179'N	85°45.692'W	H1432	11
	Galápagos	NA063-003	MCZ383302	0°46.182'N	85°54.705'W	H1432	2
Lepetodrilus tevnianus	Galápagos	NA063-007	MCZ383293	0°46.181'N	85°54.710'W	H1432	3
Lepetodrilus galriftensis	Galápagos	NA063-009	MCZ383295	0°46.174'N	85°54.698'W	H1432	14
	Galápagos	NA063-007	MCZ383293	0°46.181'N	85°54.710'W	H1432	27
	Galápagos	NA063-003	MCZ383302	0°46.182'N	85°54.704'W	H1432	7
Lepetodrilus guaymasensis	Guaymas Basin	Sonora margin	-	27°35.274'N	111°28.409'W	1562	9

Tables

Table 2. List of lepetodrilid specimens used in this study (only unique haplotypes were used in the analyses, i.e. 47 sequences).

Species	Ridge system	Latitude	GenBank acc. no.
Lepetodrilus elevatus north	EPR	21–0°N	EU306402–06[a]
	EPR	13°N	EF486414,15[b]
	EPR	9°50'N	EF486402–04[b]
Lepetodrilus elevatus south	EPR	17–21°S	EF486363,64,66–69[b]
Lepetodrilus aff. *elevatus*	EPR	21°S	GU984234–36[c]
	EPR	7–38°S	EU306407–11[a]
Lepetodrilus galriftensis	Galápagos	0°	This study
Lepetodrilus aff. *galriftensis*	EPR	9°N–23°S	EU306414–18[a]
Lepetodrilus pustulosus	EPR	13°N	GU984285[b]
	EPR	21°N–17°S	EU306457–61[a]
Lepetodrilus pustulosus	Galápagos		This study
Lepetodrilus aff. *pustulosus*	EPR	31–38°S	EU306464–68[a]
Lepetodrilus tevnianus	EPR	9°N–23°S	EU306389–93[a]
Lepetodrilus aff. *tevnianus*	Galápagos	0°	This study
	EPR	23–31°S	EU306395–99[a]
Lepetodrilus guaymasensis	Guaymas	27°N	This study
Lepetodrilus sp. *guaymas*	Guaymas, Costa Rica margin	27°N, 9°N	EU306419–23[a]
Lepetodrilus cristatus	EPR	21°N–38°S	EU306425–29[a]
	EPR	13°N	GU984295,97,98,99,300[c]
Lepetodrilus fucensis	Juan de Fuca	49–47°N	DQ228006,10,14,19,23[d]
Lepetodrilus gordensis	Gorda	42–41°N	DQ228028,42,43,65,66[d]
Gorgoleptis spiralis	EPR	7–17°S	GU984238, 39, 40, 42[c]

Abbreviation: EPR, East Pacific Rise. Publication of sequences: [a]Johnson *et al.* (2008); [b]Matabos *et al.* (2008); [c]Matabos *et al.* (2010) ; [d]Johnson *et al.* (2006).

Table 3. Genetic distance matrix calculated using the Kimura 2 Parameter model of substitutions.

Species	*Lee* C1	*Lee* C2	*Lee* C3	*Leg*	*Lguay*	*Lgord*
Lepetodrilus e. elevatus (*Lee*) C1	-					
L. e. elevatus C2	0.063	-				
L e. elevatus C3	0.081	0.058	-			
L. e. galriftensis (*Leg*)	0.079	0.074	0.086	-		
L. guaymasensis (*Lguay*)	0.090	0.075	0.083	0.096	-	
L. gordensis (*Lgord*)	0.135	0.128	0.134	0.140	0.139	-
L. fucensis	0.159	0.141	0.153	0.145	0.163	0.070

Clades: C1, Clade 1 on northern East Pacific Rise; C2, Clade 2 on southern East Pacific Rise; C3, Clade 3 on Pacific-Antarctic Ridge (see Figs 3, 4).